Proposed Journal Section: Molecular and Developmental Neuroscience

Running title: Cell cycle regulation of adult SVZ precursors

Title: Differential responses of endogenous adult mouse neural precursors to excess neuronal excitation

Tetsuji Mori[a], Taketoshi Wakabayashi[a], Yukie Hirahara[a] Yasuharu Takamori[a], Taro Koike[a], Kiyoshi Kurokawa[a], Hisao Yamada[a]

[a]Department of Anatomy & Cell Science, Kansai Medical University, 10-15 Fumizono-cho, Moriguchi, Osaka 570-8506, Japan

Corresponding author:

Tetsuji Mori, PhD

Department of Anatomy & Cell Science, Kansai Medical University, 10-15 Fumizono-cho, Moriguchi, Osaka, 570-8506, Japan

Tel: +81-6-6993-9418

Fax: +81-6-6992-2706

e-mail: morite@takii.kmu.ac.jp

Total number of pages: 53

Total number of figures: 12

Total number of tables: 0

Total number of supplemental figures: 3

Total number of words in the whole manuscript: 9704

Total number of words in the Abstract: 245

Total number of words in Introduction: 476

Key words:

Seizure, adult mouse SVZ, precursor, neurogenesis, cell cycle

Abstract

Adult neurogenesis in the subgranular zone of the hippocampus (SGZ) is enhanced by excess as well as mild neuronal excitation, such as chemoconvulsant-induced brief seizures. Because most studies of neurogenesis after seizures have focused on the SGZ, the threshold of neuronal excitation required to enhance neurogenesis in the subventricular zone (SVZ) is not clear. Therefore, we examined the responses of SVZ precursors to brief generalized clonic seizures induced by a single administration of the chemoconvulsant pentylenetetrazole (PTZ). Cell cycle progression of precursors was analyzed by systemic administration of thymidine analogues. We found that brief seizures immediately resulted in cell cycle retardation in the SVZ. However, the same effect was not seen in the SGZ. This initial cell cycle retardation in the SVZ was followed by enhanced cell cycle re-entry after the first round of mitosis, leading to precursor pool expansion, but the cell cycle retardation and expansion of the precursor pool were transient. Cell cycle progression in the PTZ-treated group returned to normal after one cell cycle. The numbers of precursors in the SVZ and new neurons in the olfactory bulb, which are descendants of SVZ precursors, were not significantly different from those in control mice more than 2 days after seizures. Because similar

effects were observed following electroconvulsive seizures, these responses are likely to be general effects of brief seizures. These results suggest that neurogenesis in the SVZ is more tightly regulated and requires stronger stimuli to be modified than that in the SGZ.

Introduction

There are two neurogenic regions in the adult mammalian brain: the subventricular zone (SVZ) and the subgranular zone (SGZ) of the hippocampus. Neural precursors, including stem cells and progenitors, reside in these regions and produce neurons throughout a mammal's lifetime. There are at least three different precursor cell types in the adult SVZ: type B, relatively quiescent stem cells; type C, transitory amplifying cells undergoing active proliferation; and type A, proliferating neuroblast cells. After sequential differentiation from type B to C to A, precursors migrate to the olfactory bulb (OB) through the rostral migratory stream (RMS) (Mori *et al.*, 2005). It is known that the precursor properties, structures, and microenvironments of neurogenic niches in the SVZ and SGZ are different. For example, the culturing conditions for and proliferation properties of these populations of cells (Walker *et al.*, 2008), their cellular compositions (Doetsch *et al.*, 1997; Kempermann *et al.*, 2004), and the instructive cues required for precursor differentiation (Suhonen *et al.*, 1996) are different. Endogenous precursors are a promising target for therapeutic strategies to replace neurons damaged by injury or neurodegenerative diseases. Understanding the mechanisms of cell cycle regulation and the differentiation of endogenous precursors is important, but these have not been

thoroughly studied.

SGZ precursors in the adult hippocampus proliferate in response to both non-harmful and mildly harmful events, such as stress, aging, learning, environmental enrichment and physical exercise, as well as strong pathological events, such as stroke, traumatic brain injuries and epileptic seizures (Fabel & Kempermann, 2008; Kernie & Parent, 2010). Epilepsy is the most common disorder of the brain and is triggered by abnormal neuronal excitation. In various animal models of epilepsy, such as kindling and status epilepticus, neurogenesis is enhanced in the hippocampus (Bengzon *et al.*, 1997; Parent *et al.*, 1997). These epilepsy models also usually exhibit neuronal cell death (Cavazos *et al.*, 1994; Kasof *et al.*, 1995).

Pentylenetetrazole (PTZ) is a chemoconvulsant that acts as a GABA-A receptor antagonist. Systemic administration of PTZ induces various types of generalized seizures in a dose-dependent manner (Andre *et al.*, 1998). Brief seizures induced by a single administration of PTZ are much milder than status epilepticus and kindling, and brief-seizure model animals show no apparent neuronal death (see references in Kasof *et al*., 1995). PTZ-induced brief seizures also dramatically enhance neurogenesis in the adult rat dentate gyrus of the hippocampus (Jiang *et al.*, 2003).

Most studies of the relationship between epilepsy or seizures and neurogenesis have

focused on the hippocampus (Bengzon *et al.*, 1997; Parent *et al.*, 1997). Although status epilepticus enhances neurogenesis in the SVZ–OB system (Parent *et al.*, 2002), like it does in the SGZ, it is unclear whether brief seizures also have an effect on adult SVZ precursors. Therefore, the purpose of this study was to examine the responses of SVZ neural precursors to brief seizures in the short and long term.

Materials and Methods

Animals

Six- or seven-week-old male ICR mice were used in all experiments. Mice were supplied by Japan SLC. Inc. (Hamamatsu, Japan). Total 208 mice were used in the present study. The experimental protocols were approved by the animal ethics committee at Kansai Medical University and were performed in accordance with the Principles of Laboratory Animal Care (NIH publication no. 85-23, revised 1985).

Drugs

5-bromo-2’-deoxyuridine (BrdU, Sigma, St. Louis, MO, USA) and PTZ (Sigma) were

dissolved in phosphate-buffered saline (PBS) at 10 mg/ml. Because of the lower solubility of 5-iodo-2'-deoxiuridine (IdU, Tokyo Kasei, Tokyo, Japan), it was dissolved in 0.014 M NaOH/PBS at 6 mg/ml. All drugs were administered intraperitoneally (IP). The dose of PTZ required to induce seizures in mice was determined before starting this study. PTZ was administered at a dose of 60 mg/kg (body weight), and only mice that exhibited brief generalized clonic seizures were used in experiments. BrdU (molecular weight = 307.1) and IdU (molecular weight = 354.1) were used to label proliferating cells. BrdU was administered at doses of 50 mg/kg and 100 mg/kg for SVZ and SGZ analysis, respectively. IdU was administered at a dose of 115.3 mg/kg, equimolar to 100 mg/kg of BrdU, for SGZ analysis.

Experimental protocol 1

Cell cycle progression, migration, and the long-term fate of SVZ precursors were analyzed after PTZ-induced seizures using the following protocol. BrdU was administered 10 minutes after PTZ administration. An identical volume of PBS was administrated to control mice. Mice were fixed at the following time points: 1, 2, 3, 4, 14, 16, 18, and 20 hours, 3 and 7 days, and 4 weeks after BrdU administration.

Experimental protocol 2

The cell cycle kinetics of SGZ precursors were analyzed by sequential administration of IdU and BrdU, as described previously (Burns & Kuan, 2005). Briefly, IdU was administered 10 minutes after PTZ administration, and an administration of BrdU followed 3 or 6 hours later. Mice were fixed 30 minutes after BrdU administration. An identical volume of PBS substituting for PTZ was administrated to control mice.

Experimental protocol 3

The number of proliferating precursors in the SVZ was analyzed after PTZ-induced seizures using the following protocol. BrdU was administered 2 or 4 days after PTZ administration. Mice were fixed 2 hours after BrdU administration. Control mice were administrated an identical volume of PBS.

Experimental protocol 4

Surplus precursors were labeled by BrdU after PTZ-induces seizures using the following protocol. BrdU was administrated 20, 24, 28, and 32 hours (total 4 administrations per animal) after PTZ administration. Control mice were administrated an identical volume of PBS. Mice were fixed 4 weeks after the last BrdU

administration.

Experimental protocol 5

Electroconvulsive seizures (ECS) were induced by applying a single shock (80V for 0.3 seconds) through the corneas without anesthetic. After electrical stimulation, mice immediately exhibited generalized clonic or tonic clonic seizures for several seconds. BrdU was administered 10 minutes after the induction of ECS. Mice were fixed 2 or 20 hours after BrdU administration.

Histological procedures

For histological analysis, mice were deeply anesthetized with pentobarbital (50 mg/kg) and perfused transcardially with PBS followed by 4% formaldehyde in PBS. The brains were removed, post-fixed with the same fixative overnight, and cryoprotected with 20% sucrose in PBS. Brains were embedded in O.C.T. compound (Sakura Fintek, Tokyo, Japan), snap frozen on dry ice, and cut transversely using a cryostat. For analysis of the SVZ and SGZ, brains were sectioned at a thickness of 30- or 16-μm as floating sections. For analysis of the OB, OBs were sectioned at a thickness of 12-μm and attached to glass slides. The sections were then processed for immunohistochemistry.

To detect BrdU, sections were pretreated with 2 M HCl for 30 minutes at room temperature followed by neutralization with 0.1 M boric acid (pH 8.5) and three washes in PBS. To detect Ki67, sections were heated at 99°C in 0.01M citrate buffer (pH 6.0) for 10 minutes. For double-immunostaining with anti-BrdU and another primary antibody, sections were incubated in a primary antibody cocktail. The following primary antibodies were used: rat monoclonal anti-BrdU (Clone BU1/75, 1:200, Abcam, Cambridge, UK), mouse monoclonal anti-BrdU (Clone B44, 1:200, BD Biosciences, San Jose, CA, USA) , rabbit anti-phosphohistone H3 (PH3) (1:600, Millipore, Billerica, MA, USA), rabbit anti-Ki67 (1:1000, Novocastra, Newcastle, UK), mouse anti-NeuN (1:200, Millipore), mouse anti-GFAP (1:800, Sigma), guinea pig anti-DCX (doublecortin, 1:2000, Millopore), sheep anti-EGF receptor (EGFR, 1:50, Millipore), goat anti-Iba1 (1:400, Abcam), and rabbit anti-calretinin (CR, 1:100, Millipore). Primary antibodies were detected using species-specific donkey secondary antibodies conjugated to Cy2 or Cy3 (1:200, Jackson ImmunoResearch, West Grove, PA, USA). To visualize nuclei, stained sections were mounted onto glass slides using a medium containing 100 mM DTT, 50% glycerol and 5 μg/ml Hoechst 33258. Apoptotic cells were detected using a TUNEL kit (Roche, Mannheim, Germany). Fluorescence images were acquired using an epifluorescent microscope (BZ-9000 with a Plan Apo 4x, NA

0.20 lens, Keyence, Osaka, Japan) or a confocal microscope (LSM510-Meta, Carl Zeiss, Oberkochen, Germany). For confocal microscopic images, a Zeiss C-Apochromat 40x/1.2w lens and pinhole aperture of 1 Airy unit was used. Voxel size was 0.45 x 0.45 x 1μm. Total 25-28 objective sections were acquired.

Quantification analysis

All animals were coded and the codes were not broken until the end of analysis to achieve unbiased quantification. Cell counting was performed on an epifluorescent microscope (x400 magnification, Axioplan2, Carl Zeiss). A Zeiss Plan-NEOFLUOR 40x/1.3 oil DIC lens was used. The SVZ was analyzed at the level of the anterior SVZ (anteroposterior (AP) 0 - 1.0 mm from the bregma). Every tenth 30-μm-thick section of the SVZ was collected and a total of three sections per animal were analyzed. For quantification of the total number of Ki67-immunopositive (+) cells in the SVZ, every tenth 16-μm-thick section was collected, and a total of six sections per animal were analyzed. For analysis of cell cycle kinetics of the SGZ, every third 30 μm-thick section was collected (AP -1.3 - -2.7 mm from the bregma) and a total of 15 sections per animal were analyzed. For quantification of the total number of Ki67+ cells in the SGZ, every other 30 μm-thick section was pooled (AP -1.5 - -2.5 mm from the bregma) and a total

of five sections per animal were randomly analyzed. For analysis of the OB, every 25th section at the center of the OB (AP 3.8 - 4.7 mm from the bregma) was collected and a total of three sections per animal were analyzed. Stereotaxis coordinates are based on those of Paxinos and Franklin (Paxinos & Franklin, 2001). Percentages and total numbers are expressed as average values per animal. All data are presented as the average ± standard error of the mean (SEM). In all experimental conditions, more than three animals were analyzed. Levels of significance were determined using the two-tailed unpaired Welch's *t*-test to compare two groups, and one-way ANOVA to compare more than three groups. Statistical significance was set at $P < 0.05$. Statistical analyses were performed by R.

Results

PTZ-induced brief seizures

In a pilot experiment, the dose of PTZ necessary to induce brief generalized clonic seizures with a twisted posture and falling that lasted for several seconds was determined. An IP injection of 60 mg/kg PTZ induced brief seizures in 69.1% of mice,

and the mortality rate was 2.5% (n = 81). Brief seizures were induced within 5 minutes in 89.3% of the mice showing seizures (n = 56). Only mice that exhibited brief seizures of this type were used. There was no significant increase in the amount of neuronal death, as determined by the pyknotic nuclear morphology revealed by Hoechst 33258 nuclei staining (data not shown) and TUNEL staining in the SVZ of PTZ-treated mice (17.80 ± 2.71 in the control vs. 27.40 ± 3.86 in the PTZ, n = 5, two-tailed Welch's t-test, $t_{7.177}$ = -2.037, P = 0.081) (Supplemental Figure 1). These results are consistent with those of other studies (see references in Kasof *et al*., 1995).

Cell cycle retardation of SVZ precursors immediately after brief seizures

Experimental protocol 1 was used to assess cell cycle progression immediately after brief seizures. S phase precursors are labeled by BrdU. When these cells enter the G2/M phase, they become positive for PH3, a G2/M phase-specific marker (Hendzel *et al.*, 1997). The anti-PH3 antibody stain nuclei of mitotic cells, but the staining patterns are different between G2 phase (punctate signals in the nuclei) and M phase (intense and even signal in the nuclei or highly organized chromosomes) (Hendzel *et al.*, 1997). In the present study, we counted only M phase cells to simplify quantification. Thus, the temporal change in the ratio of BrdU and PH3 double-positive cells among all PH3+

cells ((BrdU+, PH3+)/PH3+) indicates the progression of BrdU+ cells into the M phase (Figure 1 A–D).

First, BrdU labeling efficiency was comparable between the control and PTZ-treated groups at 1 hour (1115.20 ± 53.66 cells in the control vs. 1112.20 ± 29.81 cells in the PTZ; $t_{6.255} = 0.635$, $P = 0.549$), and at 2 hours (1789.40 ± 69.55 cells in the control vs. 1845.20 ± 67.20 cells in the PTZ; $t_{7.991} = -0.577$, $P = 0.580$) (Figure 2A). Moreover average numbers of PH3+ cells were not significantly different at each time point between the control and PTZ-treated groups ($t_{6.558} = 1.977$, $t_{6.800} = 1.263$, $t_{6.766} = 1.016$, $t_{7.815} = 0.131$, $t_8 = -1.051$, $t_{7.615} = -0.836$, $t_{7.198} = 0.815$, and $t_{7.592} = -0.193$, and $P = 0.089$, 0.242, 0.343, 0.899, 0.353, 0.427, 0.442, and 0.852 at 1, 2, 3, 4, 14, 16, 18 and 20 hours respectively) (Figure 2B). The (BrdU+, PH3+)/PH3+ ratios were plotted against the interval between BrdU administration and fixation. In the control group, the (BrdU+, PH3+)/PH3+ ratio reached about 70% 2 hours after BrdU administration (Figure 2C) and continued to increase about 5% per hour.

In the PTZ-treated group, the (BrdU+, PH3+)/PH3+ ratio was significantly lower than in the control group at 1 hour (13.76 ± 3.43% in the control vs. 1.41 ± 0.68% in the PTZ; $t_{4.310} = 3.533$, $P = 0.024$) and 2 hours (71.39 ± 2.74% in the control vs. 57.98 ± 4.09% in the PTZ; $t_{6.989} = 2.720$, $P = 0.030$). But the (BrdU+, PH3+)/PH3+ ratios were

not significantly different between the control and PTZ-treated group at 3 hours (76.80 ± 1.66% in the control vs. 72.42 ± 2.18% in the PTZ; $t_{7.465} = 1.596$, $P = 0.155$) and at 4 hours (81.60 ± 0.58% in the control vs. 76.95 ± 2.60% in the PTZ; $t_8 = 1.728$, $P = 0.159$) (Figure 2C). This result shows that there is obvious cell cycle retardation in PTZ-treated mice immediately after seizures.

Next, we followed cell cycle progression after the first round of mitosis. In control mice, the (BrdU+, PH3+)/PH3+ ratio decreased to about 8% 14 and 16 hours after BrdU administration. The ratio began to increase at 18 hours, suggesting that BrdU-labeled precursors had entered a second M phase (Figure 1C, 1D, and Figure 2C). In the PTZ-treated group, the (BrdU+, PH3+)/PH3+ ratio also began to increase at 18 hours (Figure 2C). However, at the 14-, 16-, 18-, and 20-hour time points, the (BrdU+, PH3+)/PH3+ ratios were not significantly different between the control and PTZ-treated groups (8.52 ± 0.60% in the control vs. 10.70 ± 0.78% in the PTZ; $t_{7.533} = -2.211$, $P = 0.058$ at 14 hours, 8.77 ± 1.16% in the control vs. 7.56 ± 0.57% in the PTZ; $t_{5.809} = 0.945$, $P = 0.381$ at 16 hours, 20.10 ± 3.14% in the control vs. 17.32 ± 2.04% in the PTZ; $t_{6.866} = 0.744$, $P = 0.481$ at 18 hours, and 37.68 ± 3.64% in the control vs. 35.34 ± 0.70% in the PTZ; $t_{4.297} = 0.630$, $P = 0.563$ at 20 hours). These data show that the cell cycle length of normal adult SVZ precursors is about 17 hours, and that cell cycle

progression in the PTZ-treated group returned to control levels at the second M phase.

Normal cellular composition of the SVZ after brief seizures

Brief seizures affect cell cycle progression of the SVZ precursors as shown above. Each type of the SVZ precursors, type A (DCX+), B (GFAP+), and C (EGFR+) cells, has different cell cycle length. Moreover seizures can activate microglia (Iba1+) (Vezzani *et al.*, 2011). Thus we examined the cellular composition of the proliferating cells in the SVZ after brief seizures by calculating the ratio of the cell type marker and PH3 double + cells among all PH3+ cells ((marker+, PH3+)/PH3+).

Because DCX and EGFR expressions partially overlapped each other (Figure 3A, arrows), type A and C cells were stained with the same color (red, Figure 3B), and the ratio of (EGFR + and/or DCX+, PH3+)/PH3+ was calculated. Vast majority of the proliferating cells was type A and C (total about 85%), and type B cells were about 5% (Figure 3C and 3E), consisting with a previous report (Doetsch *et al.*, 1997). There was virtually no proliferating Iba1+ microglia (Figure 3D and 3E). Cellular composition of the proliferating cells in the SVZ did not change significantly between the control and PTZ-treated groups (EGFR, $F_{4, 20} = 1.285$, $P = 0.309$; EGFR+DCX, $F_{4, 20} = 2.249$, $P = 0.100$; GFAP, $F_{4, 20} = 0.757$, $P = 0.565$; Iba1, $F_{4, 20} = 1.427$, $P = 0.262$)) (Figure 3E).

These data show that brief seizures do not change cellular composition of proliferating precursors in the SVZ.

Normal cell cycling of SGZ precursors immediately after brief seizures

The SGZ precursors respond to proliferate after several days in various seizure models (Bengzon *et al.*, 1997; Parent *et al.*, 1997; Jiang *et al.*, 2003; Bolteus & Bordey, 2004; Park *et al.*, 2006), but their response is unclear immediately after seizures. The SGZ contains far fewer proliferating precursors than the SVZ, and the number of PH3+ cells is insufficient to analyze cell cycle stages precisely using protocol 1 (less than three PH3+ cells per 30-μm-thick section; data not shown). In a preliminary experiment, single administration of 100 mg/kg BrdU revealed about 12 BrdU+ SGZ precursors per 30-μm-thick section (data not shown). Thus, we quantified IdU- and BrdU-labeled SGZ precursors in 15 sections per animal using protocol 2 to analyze cell cycle progression in the SGZ after brief seizures. First, IdU was administered to label S phase cells. BrdU was then administered after 3 or 6 hours. It is known that rat anti-BrdU antibody (clone BU1/75) recognizes BrdU, but not IdU, and that mouse anti-BrdU (clone B44) recognizes both BrdU and IdU (Burns & Kuan, 2005). Thus, the ratio of IdU-only + cells among all + cells (IdU-only + cells, IdU and BrdU double + cells, and BrdU-only

+ cells) increases to ~50% until all IdU-labeled cells exit S phase (Figure 4A and Supplemental Figure 2). Using this double thymidine analogue labeling method, Burns et al. estimated that the S phase of adult mouse SGZ precursors lasts for about 6 hours (Burns & Kuan, 2005). In the present study, the IdU-only +/all + cell ratios were about 20% and 45% at 3 and 6 hours respectively, and they were consistent with previous report (Burns & Kuan, 2005). There was no significant difference between the control and PTZ-treated groups (20.63 ± 1.58% in the control vs. 22.02 ± 1.71% in the PTZ; $t_{5.964}$ = -0.599, P = 0.571 at 3 hours, and 45.52 ± 1.02% in the control vs. 46.97 ± 2.53% in the PTZ; $t_{3.946}$ = -0.532, P = 0.623 at 6 hours) (Figure 4B). This result shows that there is no cell cycle retardation in the SGZ immediately after brief seizures, unlike in the SVZ.

Enhanced precursor proliferation in the SGZ after brief seizures

Jiang et al. showed that precursor proliferation in the adult rat SGZ was enhanced between 3 to 14 days after brief seizures induced by a single administration of PTZ, and it peaked on the third day (Jiang *et al.*, 2003). We also analyzed precursor proliferation in the adult mouse SGZ by quantifying Ki67, a marker of proliferating cells, + cells after brief seizures. At 1 hour, the number of Ki67+ cells was not significantly different

between the control and PTZ-treated group (182.80 ± 13.17 in the control vs. 156.80 ± 8.77 in the PTZ; $t_{6.964}$ = 1.642, P = 0.144) (Figure 5A). At 3 days, the number of Ki67+ cells in the PTZ-treated mice had significantly higher than the control mice (179.00 ± 13.18 in the control vs. 260.80 ± 15.05 in the PTZ; $t_{7.863}$ = -4.090, P = 0.0035) (Figure 5A and 5B). But at 7 days, the number of Ki67+ cells was not significantly different between the control and PTZ-treated group (165.00 ± 13.18 in the control vs. 136.80 ± 4.49 in the PTZ; $t_{4.915}$ = 2.025, P = 0.099) (Figure 5A). These data show that precursor proliferation in the adult mouse SGZ is also enhanced by brief seizures(Jiang *et al.*, 2003)(Jiang *et al.*, 2003)(Jiang *et al.*, 2003).

Transient expansion of the SVZ precursor pool after brief seizures

In general, strong pathological events that result in neuronal death, such as status epilepticus, stroke, and certain brain injuries, expand the precursor pool and promote neurogenesis in the SVZ and the SGZ (Parent *et al.*, 2002; Zhang *et al.*, 2006). We examined whether PTZ-induced brief seizures, which are much less traumatic events than status epilepticus, also lead to expansion of the precursor pool. Importantly, as described above, cell cycle retardation occurs in the early phase.

We compared the numbers of cells undergoing cycle re-entry between the control and

PTZ-treated groups 20 hours after BrdU administration by calculating the ratio of Ki67 and BrdU double + cells among all BrdU+ cells ((Ki67+, BrdU+)/BrdU+) using experimental protocol 1 (Figure 6A). Ki67 is expressed throughout all phases of the cell cycle and its protein expression level decreases rapidly after cells exit the cell cycle (Mori *et al.*, 2009). The (Ki67+, BrdU+)/BrdU+ ratio in the PTZ seizure group was significantly higher than that in the control group (63.86 ± 3.33% in the control vs. 77.02 ± 0.33% in the PTZ; $t_{5.100}$ = -3.933, P = 0.011) (Figure 6B). This result shows that approximately 1.2-fold more precursors re-entered the cell cycle in the first round of mitosis in the PTZ-treated group compared with the control group. Consistent with this data, the total number of Ki67+ cells was also about 1.2-fold higher in the PTZ-treated group than in the control group (4570.4 ± 201.36 cells in the control vs. 5588 ± 96.15 cells in the PTZ; $t_{5.734}$ = -4.560, P = 0.0039) (Figure 6C). However, at 20 hours, number of PH3+ cells was not significantly different between the control and the PTZ-treated group (Figure 2B). Because it suggests that surplus precursors are still in the G1 and S phases at 20 hours, we followed the number of PH3+ cells after 20 hours. The numbers of PH3+ cells were significantly higher in the PTZ-treated group than in the control group at 22 hours (127.40 ± 7.10 cells in the control vs. 176.40 ± 12.85 cells in the PTZ; $t_{6.237}$ = -3.338, P = 0.016) and 26 hours (127.00 ± 9.42 cells in the control vs. 160.40 ±

9.70 cells in the PTZ; $t_{7.993}$ = -2.470, P = 0.039). But the numbers of PH3+ cells were not significantly different between the control and PTZ-treated group at 30 hours (136.60 ± 7.68 cells in the control vs. 149.80 ± 6.28 cells in the PTZ; $t_{7.697}$ = -1.331, P = 0.220) and 36 hours (122.60 ± 6.71 cells in the control vs. 145.20 ± 9.88 cells in the PTZ; $t_{7.044}$ = -1.892, P = 0.100) (Figure 6D).

Next, using experimental protocol 3, we examined whether SVZ precursor expansion is a long-term process. The total number of BrdU+ cells was plotted against the interval between PTZ and BrdU administration. There were no significant differences between controls and experimental mice at 2 days (1796.40 ± 37.39 cells in the control vs. 1818.00 ± 103.00 cells in the PTZ; $t_{5.036}$ = -0.197, P = 0.851) and 4 days (1802.40 ± 97.19 cells in the control vs. 1670.20 ± 74.19 cells in the PTZ; $t_{7.480}$ = 1.081, P = 0.315) after PTZ administration (Figure 6E).

These data suggest that precursor pool expansion in the SVZ immediately after brief seizures is transient and does not continue after the first round of mitosis.

Long-term effects of PTZ-induced seizures on adult neurogenesis in the SVZ–OB system

The mouse SVZ precursors migrate to the core of the OB taking about 1 week (Lois &

Alvarez-Buylla, 1994) and differentiate into mature granule or peri-glomerular neurons.

First, using experimental protocol 1, we addressed a possibility that brief seizures affect migration of precursors. There were few BrdU+ cells in the OB immediately after BrdU administration, but BrdU labeled precursors migrated and accumulated in the core of the OB over time (Figure 7A and 7B). After precursors reached to the OB, they migrated radially and differentiated into mature neurons (Figure 7C and Supplemental Figure 3). The number of BrdU+ cells was not significantly different between the control and PTZ-treated groups 3 days (728.67 ± 24.17 cells in the control vs. 756.67 ± 30.47 cells in the PTZ; $t_{3.803}$ = -0.730, P = 0.511) and 7 days after brief seizures (2245.67 ± 79.81 cells in the control vs. 2162.67 ± 107.73 cells in the PTZ; $t_{3.687}$ = 0.619, P = 0.569) (Figure 7D).

Second, we examined whether PTZ-induced brief seizures change the differentiation fate of precursors in the SVZ–OB system in mice sacrificed at the 4-week time point. We examined neuronal differentiation of the SVZ precursors using protocol 1 by calculating the ratio of NeuN and BrdU double + cells among all BrdU+ cells ((NeuN+, BrdU+)/BrdU+). The total number of BrdU+ cells in the OB was not significantly different between the controls and PTZ-treated animals (533.00 ± 148.06 cells in the control vs. 523.00 ± 118.96 cells in the PTZ; $t_{5.734}$ = 0.053, P = 0.960) (Figure 8A). And

there was no significant difference in the (NeuN+, BrdU+)/BrdU+ ratio between the control and PTZ-treated groups (77.74 ± 2.26% in the control vs. 75.59 ± 0.45% in the PTZ; $t_{3.240} = 0.932$, $P = 0.420$,) (Figure 8B).

Third, using experimental protocol 4, we labeled surplus precursors in the SVZ with BrdU and their final positions in the OB were examined. The total number of BrdU+ cells was not significantly different between the control and PTZ-treated groups (3079.33 ± 236.21 cells in the control vs. 3112.67 ± 271.27 cells in the PTZ; $t_{3.926} = -0.093$, $P = 0.931$). Also the numbers of BrdU+ cells in the granular layer of the OB (GrO) (2529.33 ± 179.90 cells in the control vs. 2541.67 ± 231.90 cells in the PTZ; $t_{3.767} = -0.042$, $P = 0.968$) and in the glomerular layer (Gl) (550.00 ± 58.11 cells in the control vs. 571.00 ± 40.60 cells in the PTZ; $t_{3.577} = -0.296$, $P = 0.782$) were not significantly different between the control and PTZ-treated group (Figure 8C). Moreover, the morphologies of BrdU and calretinin (CR) double + mature granular neurons in the control and the PTZ-treated mice were similar to each other (Supplemental Figure 3C). These results show that brief seizures do not affect neurogenesis in the SVZ-OB system, even though transient expansion of the SVZ precursor pool immediately after seizures.

Electroconvulsion has effects similar to PTZ-induced seizures on SVZ precursors

It is known that GABA-A receptor signals regulate precursor proliferation (LoTurco *et al.*, 1995; Fiszman *et al.*, 1999; Liu *et al.*, 2005; Fukui *et al.*, 2008). Because PTZ is an antagonist of the GABA-A receptor, it is possible that the cell cycle retardation and the expansion of the precursor pool we observed in PTZ-treated mice were driven by PTZ rather than by general effects of the seizures. To clarify this issue, using experimental protocol 5, we performed the same analyses following induction of an electroconvulsive seizure (ECS). The (BrdU+, PH3+)/PH3+ ratio in the ECS group was significantly lower than that in the control group at 2 hours (71.39 ± 2.74% in the control vs. 57.96 ± 3.35% in the ECS; ($t_{7.700}$ = 3.100, P = 0.015) (Figure 9A).

At the 20-hour time point, the (Ki67+, BrdU+)/BrdU+ ratio in the ECS group was significantly higher than that in the control group (63.86 ± 3.33% in the control vs. 77.35 ± 1.26% in the ECS; $t_{6.366}$ = -3.790, P = 0.007) (Figure 9B). These results show that PTZ-induced seizures and ECS have similar effects on the cell cycle progression of SVZ precursors and that cell cycle retardation and expansion of the precursor pool are general effects of seizures.

Discussion

It is known that status epilepticus affects the proliferation of precursors in the adult SGZ (Bengzon *et al.*, 1997; Parent *et al.*, 1997), but few studies have focused on the SVZ (Parent *et al.*, 2002). Additionally, there has been no study examining the responses of SVZ precursors to brief seizures, a much milder stimulus than status epilepticus. In addition, there have been no analyses of early phase responses.

Cell cycle length in mouse SVZ precursors

Understanding cell cycle kinetics is the first step toward elucidating the mechanisms underlying adult neurogenesis. The mouse has become a more useful model animal for biological studies than the rat because of the many lines of transgenic mice that are now available. The cell cycle lengths of neuronal precursors in the adult rat SVZ and SGZ and the adult mouse SGZ have already been described by many research groups (Hayes & Nowakowski, 2002; Zhang *et al.*, 2006; Mandyam *et al.*, 2007), but there have been few studies of the adult mouse SVZ (Morshead & van der Kooy, 1992).

The present study found that the length of the cell cycle in adult mouse SVZ precursors is about 17 hours. This is much longer than the 12.7 hours estimated by Morshead et al. (Morshead & van der Kooy, 1992). There are two possible reasons for this difference.

First, we used ICR mice while Morshead et al. used CD1 mice. Precursor cells in different mouse strains could have different cell cycle lengths. Second, we analyzed the entire anterior SVZ around the lateral ventricle, while Morshead et al. analyzed only the dorsolateral region. The cellular composition of precursors varies along the antero-posterior (Doetsch *et al.*, 1997) and dorso-ventral (Sundholm-Peters *et al.*, 2004) axes, and cell cycle length is different in each SVZ precursor type (Mori *et al.*, 2005). Because the BrdU labeling method cannot discriminate between precursor cell types, analysis of different regions could result in variations in estimated cell cycle length.

In the normal mice, the (BrdU+, PH3+)/PH3+ ratio dramatically increased from 1 to 2 hours, and continued to slightly increase about 5% per hour. This suggests that there are at least two precursor populations with different cycling speed. Indeed, cell cycle length of type B cell is much longer than type A and C cell (Mori *et al.*, 2005), and present study shows that the ratio of type B (GFAP+) cells among total proliferating cells was very low. Thus, the G2/M phase of majority of cycling cells in the adult mouse SVZ lasts about 2 hours.

The estimated lengths of the cell cycle (17 hours) and G2/M phase (about 2 hours) in the present study are close to those in adult rats (19 and 2 hours, respectively) (Zhang *et al.*, 2006), while the cell cycle length in the adult mouse SGZ (14 hours) is much shorter

than that in the adult rat SGZ (24.7 hours) (Hayes & Nowakowski, 2002; Zhang *et al.*, 2006; Mandyam *et al.*, 2007). This suggests that, even in different species, the cell cycle kinetics in the adult SVZ is conserved.

Early phase response of SVZ precursors after brief seizures

It is known that GABA-A receptor signals regulate precursor proliferation, but their effects are controversial. These signals can act as both positive (Fiszman *et al.*, 1999; Fukui *et al.*, 2008) and negative regulators (LoTurco *et al.*, 1995; Liu *et al.*, 2005). This inconsistency is likely to be dependent on the experimental conditions. Regardless, it is likely that irregular cell cycle progression after brief seizures is independent of PTZ and that it is a general effect of seizures because similar effects were observed both in PTZ-treated and ECS groups.

Because cell cycle retardation occurs immediately after brief seizures, it is unlikely that *de novo* protein synthesis is responsible for cell cycle retardation. Depolarization induced by AMPA/kainate receptors negatively regulates the proliferation of embryonic cortical precursors (LoTurco *et al.*, 1995). In addition, AMPA/kainite receptors and mGluR5 are expressed in migrating progenitors in the adult SVZ (Platel *et al.*, 2008). Thus, it is possible that seizures enhance glutamate release from neurons and astrocytes

and that the activation of glutamate receptors inhibits cell cycle progression. Moreover, nitric oxide (NO) generation is immediately upregulated following seizures (Kaneko *et al.*, 2002). Because NO has an inhibitory effect on the proliferation of adult SVZ precursors (Moreno-Lopez *et al.*, 2004), NO is another candidate molecule responsible for cell cycle retardation immediately after brief seizures.

Late phase responses of SVZ precursors after brief seizures

The expansion of the SVZ precursor pool after brief seizures is not dependent on PTZ, as discussed above. Moreover, because the half-life of PTZ is estimated to be about 2 hours *in vivo* (see references in Park *et al*., 2006), late phase responses must be due to the general effects of seizures.

Because brief seizures did not affect migration of the precursors, transient expansion of precursor pool could not be a result of a migration jam. Extracellular microenvironmental cues are important for proliferation and differentiation of precursor cells (Suhonen *et al.*, 1996). Neuronal depolarization enhances the activity and gene expression of matrix metalloproteinase (MMP)-9 and several tissue inhibitors of matrix metalloproteinases (TIMPs), resulting in degradation and remodeling of the extracellular matrix (von Gertten *et al.*, 2003; Gursoy-Ozdemir *et al.*, 2004). Because

MMPs induce precursor proliferation *in vitro* (Barkho *et al.*, 2008), it is possible that microenvironmental changes lead to precursor pool expansion after brief seizures.

Another possibility is that seizures enhance the expression of some growth factors responsible for precursor proliferation and/or survival. In the hippocampus, status epilepticus, kindling, and synaptic activation upregulates expression of several growth factors including bFGF, BDNF (Isackson *et al.*, 1991; Indulekha *et al.*, 2010), and growth hormone (Kato *et al.*, 2009). These growth factors are involved in the neurogenesis, proliferation and survival of precursors (Kuhn *et al.*, 1997; Benraiss *et al.*, 2001). However, there was no significant increase in the number of BrdU+ cells in the OB after brief seizures. Because brief seizures are much milder than status epilepticus and kindling, these microenvironmental changes and upregulation of growth factors could be transient.

Under normal conditions, many precursors in the SVZ–OB system are eliminated by programed cell death (PCD) before they completely mature (Biebl *et al.*, 2000). Surplus precursors generated by brief seizures might also die, although no obvious cell loss was observed by TUNEL staining. There are at least three possibilities. (1) Surplus precursors are eliminated by apoptosis gradually, making it difficult to detect significant increases in the number of apoptotic cells in PTZ-treated mice by TUNEL staining. (2)

They die by autophagy, a type of PCD that occurs normally during development (Fimia *et al.*, 2007). Indeed, growth factor withdrawal induces autophagy in cultured hippocampal neural stem cells (Yu *et al.*, 2008). Thus, transient upregulation of growth factors after brief seizures could lead to autophagy of surplus precursors. (3) Brief seizures might enhance phagocytic activity of DCX+ cells, a recently identified function of DCX+ precursors (Lu *et al.*, 2011). Unfortunately autophagy and phagocytosis can not be detected by TUNEL staining. Further studies are needed to elucidate the mechanisms underlying cell cycle regulation and survival after brief seizures.

Seizures and neurogenesis: differential responses between the SVZ and the SGZ

We detected cell cycle retardation in the SVZ, but not in the SGZ immediately after seizures. In addition, in a similar experiment, Jiang et al. showed that brief seizures enhanced precursor proliferation in the SGZ that peaked on the third day after induction of seizures, and an increased number of BrdU+ mature neurons in the dentate gyrus (Jiang *et al.*, 2003). Moreover, neuronal excitation induces neuronal differentiation of adult hippocampal neural precursor cells *in vitro* culture system (Deisseroth *et al*., 2004; Babu *et al*., 2009). These findings are in sharp contrast with the transient SVZ precursor pool expansion demonstrated in the present study. These differences between the SVZ

and the SGZ might arise from differences in the precursor properties or the microenvironments of the two neurogenic regions. Indeed, there is some evidence to suggest that these factors vary between the SVZ and the SGZ (Suhonen *et al.*, 1996; Walker *et al.*, 2008).

It is still unclear whether neuronal death is necessary for enhanced neurogenesis after seizures. Several studies suggest that neuronal death might not be required for enhanced neurogenesis in the SGZ after repeated seizures and ischemia (Jin *et al.*, 2001; Park *et al.*, 2006). On the other hand, our results suggest that, in the adult SVZ, strong events that can induce obvious neuronal death might be needed for the induction of differentiation and survival of precursors. Indeed, status epilepticus enhances neurogenesis in the SVZ–OB system (Parent *et al.*, 2002).

In summary, we demonstrated that brief seizures resulted in cell cycle retardation in the adult SVZ immediately after stimulation. This inhibition was followed by a transient expansion of the precursor pool. Brief seizures did not increase the number of new neurons in the OB. Moreover, SVZ and SGZ precursors responded differently to brief seizures, and neurogenesis in the SVZ–OB system was tightly regulated.

Acknowledgments

This study was supported by Grants-in-Aid for Scientific Research (C) from the Japan Society for the Promotion of Science (T. M.), the Research Grant D from Kansai Medical University (T. M.), the Kobayashi Magobe Memorial Medical Foundation (T. M.), and the “Academic Frontier” project for Private Universities: a matching fund subsidy from the Ministry of Education, Culture, Sports, Science and Technology of Japan (H. Y.). The authors of this article declare no conflicts of interest.

References

Andre, V., Pineau, N., Motte, J.E., Marescaux, C. & Nehlig, A. (1998) Mapping of neuronal networks underlying generalized seizures induced by increasing doses of pentylenetetrazol in the immature and adult rat: a c-Fos immunohistochemical study. *Eur J Neurosci*, **10**, 2094-2106.

Barkho, B.Z., Munoz, A.E., Li, X., Li, L., Cunningham, L.A. & Zhao, X. (2008) Endogenous matrix metalloproteinase (MMP)-3 and MMP-9 promote the differentiation and migration of adult neural progenitor cells in response to chemokines. *Stem Cells*, **26**, 3139-3149.

Bengzon, J., Kokaia, Z., Elmer, E., Nanobashvili, A., Kokaia, M. & Lindvall, O. (1997) Apoptosis and proliferation of dentate gyrus neurons after single and intermittent limbic seizures. *Proc Natl Acad Sci U S A*, **94**, 10432-10437.

Benraiss, A., Chmielnicki, E., Lerner, K., Roh, D. & Goldman, S.A. (2001) Adenoviral brain-derived neurotrophic factor induces both neostriatal and olfactory neuronal

recruitment from endogenous progenitor cells in the adult forebrain. *J Neurosci*, **21**, 6718-6731.

Biebl, M., Cooper, C.M., Winkler, J. & Kuhn, H.G. (2000) Analysis of neurogenesis and programmed cell death reveals a self-renewing capacity in the adult rat brain. *Neurosci Lett*, **291**, 17-20.

Bolteus, A.J. & Bordey, A. (2004) GABA release and uptake regulate neuronal precursor migration in the postnatal subventricular zone. *J Neurosci*, **24**, 7623-7631.

Burns, K.A. & Kuan, C.Y. (2005) Low doses of bromo- and iododeoxyuridine produce near-saturation labeling of adult proliferative populations in the dentate gyrus. *Eur J Neurosci*, **21**, 803-807.

Cavazos, J.E., Das, I. & Sutula, T.P. (1994) Neuronal loss induced in limbic pathways by kindling: evidence for induction of hippocampal sclerosis by repeated brief seizures. *J Neurosci*, **14**, 3106-3121.

Doetsch, F., Garcia-Verdugo, J.M. & Alvarez-Buylla, A. (1997) Cellular composition and three-dimensional organization of the subventricular germinal zone in the adult mammalian brain. *J Neurosci*, **17**, 5046-5061.

Fabel, K. & Kempermann, G. (2008) Physical activity and the regulation of neurogenesis in the adult and aging brain. *Neuromolecular Med*, **10**, 59-66.

Fimia, G.M., Stoykova, A., Romagnoli, A., Giunta, L., Di Bartolomeo, S., Nardacci, R., Corazzari, M., Fuoco, C., Ucar, A., Schwartz, P., Gruss, P., Piacentini, M., Chowdhury, K. & Cecconi, F. (2007) Ambra1 regulates autophagy and development of the nervous system. *Nature*, **447**, 1121-1125.

Fiszman, M.L., Borodinsky, L.N. & Neale, J.H. (1999) GABA induces proliferation of immature cerebellar granule cells grown in vitro. *Brain Res Dev Brain Res*, **115**, 1-8.

Fukui, M., Nakamichi, N., Yoneyama, M., Yoshida, K., Ozawa, S., Kitayama, T.,

Nakamura, N., Taniura, H. & Yoneda, Y. (2008) Up-regulation of ciliary neurotrophic factor receptor expression by GABAA receptors in undifferentiated neural progenitors of fetal mouse brain. *J Neurosci Res*, **86**, 2615-2623.

Gursoy-Ozdemir, Y., Qiu, J., Matsuoka, N., Bolay, H., Bermpohl, D., Jin, H., Wang, X., Rosenberg, G.A., Lo, E.H. & Moskowitz, M.A. (2004) Cortical spreading depression activates and upregulates MMP-9. *J Clin Invest*, **113**, 1447-1455.

Hayes, N.L. & Nowakowski, R.S. (2002) Dynamics of cell proliferation in the adult dentate gyrus of two inbred strains of mice. *Brain Res Dev Brain Res*, **134**, 77-85.

Hendzel, M.J., Wei, Y., Mancini, M.A., Van Hooser, A., Ranalli, T., Brinkley, B.R., Bazett-Jones, D.P. & Allis, C.D. (1997) Mitosis-specific phosphorylation of histone H3 initiates primarily within pericentromeric heterochromatin during G2 and spreads in an ordered fashion coincident with mitotic chromosome condensation. *Chromosoma*, **106**, 348-360.

Indulekha, C.L., Sanalkumar, R., Thekkuveettil, A. & James, J. (2010) Seizure induces activation of multiple subtypes of neural progenitors and growth factors in hippocampus with neuronal maturation confined to dentate gyrus. *Biochem Biophys Res Commun*, **393**, 864-871.

Isackson, P.J., Huntsman, M.M., Murray, K.D. & Gall, C.M. (1991) BDNF mRNA expression is increased in adult rat forebrain after limbic seizures: temporal patterns of induction distinct from NGF. *Neuron*, **6**, 937-948.

Jiang, W., Wan, Q., Zhang, Z.J., Wang, W.D., Huang, Y.G., Rao, Z.R. & Zhang, X. (2003) Dentate granule cell neurogenesis after seizures induced by pentylenetrazol in rats. *Brain Res*, **977**, 141-148.

Jin, K., Minami, M., Lan, J.Q., Mao, X.O., Batteur, S., Simon, R.P. & Greenberg, D.A. (2001) Neurogenesis in dentate subgranular zone and rostral subventricular zone after focal cerebral ischemia in the rat. *Proc Natl Acad Sci U S A*, **98**, 4710-4715.

Kaneko, K., Itoh, K., Berliner, L.J., Miyasaka, K. & Fujii, H. (2002) Consequences of nitric oxide generation in epileptic-seizure rodent models as studied by in vivo EPR. *Magn Reson Med*, **48**, 1051-1056.

Kasof, G.M., Mandelzys, A., Maika, S.D., Hammer, R.E., Curran, T. & Morgan, J.I. (1995) Kainic acid-induced neuronal death is associated with DNA damage and a unique immediate-early gene response in c-fos-lacZ transgenic rats. *J Neurosci*, **15**, 4238-4249.

Kato, K., Suzuki, M., Kanno, H., Sekino, S., Kusakabe, K., Okada, T., Mori, T., Yoshida, K. & Hirabayashi, Y. (2009) Distinct role of growth hormone on epilepsy progression in a model of temporal lobe epilepsy. *J Neurochem*, **110**, 509-519.

Kempermann, G., Jessberger, S., Steiner, B. & Kronenberg, G. (2004) Milestones of neuronal development in the adult hippocampus. *Trends Neurosci*, **27**, 447-452.

Kernie, S.G. & Parent, J.M. (2010) Forebrain neurogenesis after focal Ischemic and traumatic brain injury. *Neurobiol Dis*, **37**, 267-274.

Kuhn, H.G., Winkler, J., Kempermann, G., Thal, L.J. & Gage, F.H. (1997) Epidermal growth factor and fibroblast growth factor-2 have different effects on neural progenitors in the adult rat brain. *J Neurosci*, **17**, 5820-5829.

Liu, X., Wang, Q., Haydar, T.F. & Bordey, A. (2005) Nonsynaptic GABA signaling in postnatal subventricular zone controls proliferation of GFAP-expressing progenitors. *Nat Neurosci*, **8**, 1179-1187.

Lois, C. & Alvarez-Buylla, A. (1994) Long-distance neuronal migration in the adult mammalian brain. *Science*, **264**, 1145-1148.

LoTurco, J.J., Owens, D.F., Heath, M.J., Davis, M.B. & Kriegstein, A.R. (1995) GABA and glutamate depolarize cortical progenitor cells and inhibit DNA synthesis. *Neuron*, **15**, 1287-1298.

Lu, Z., Elliott, M.R., Chen, Y., Walsh, J.T., Klibanov, A.L., Ravichandran, K.S. & Kipnis, J. (2011) Phagocytic activity of neuronal progenitors regulates adult

neurogenesis. *Nat Cell Biol*, **13**, 1076-1083.

Mandyam, C.D., Harburg, G.C. & Eisch, A.J. (2007) Determination of key aspects of precursor cell proliferation, cell cycle length and kinetics in the adult mouse subgranular zone. *Neuroscience*, **146**, 108-122.

Moreno-Lopez, B., Romero-Grimaldi, C., Noval, J.A., Murillo-Carretero, M., Matarredona, E.R. & Estrada, C. (2004) Nitric oxide is a physiological inhibitor of neurogenesis in the adult mouse subventricular zone and olfactory bulb. *J Neurosci*, **24**, 85-95.

Mori, T., Buffo, A. & Gotz, M. (2005) The novel roles of glial cells revisited: the contribution of radial glia and astrocytes to neurogenesis. *Curr Top Dev Biol*, **69**, 67-99.

Mori, T., Wakabayashi, T., Takamori, Y., Kitaya, K. & Yamada, H. (2009) Phenotype analysis and quantification of proliferating cells in the cortical gray matter of the adult rat. *Acta Histochem Cytochem*, **42**, 1-8.

Morshead, C.M. & van der Kooy, D. (1992) Postmitotic death is the fate of constitutively proliferating cells in the subependymal layer of the adult mouse brain. *J Neurosci*, **12**, 249-256.

Parent, J.M., Valentin, V.V. & Lowenstein, D.H. (2002) Prolonged seizures increase proliferating neuroblasts in the adult rat subventricular zone-olfactory bulb pathway. *J Neurosci*, **22**, 3174-3188.

Parent, J.M., Yu, T.W., Leibowitz, R.T., Geschwind, D.H., Sloviter, R.S. & Lowenstein, D.H. (1997) Dentate granule cell neurogenesis is increased by seizures and contributes to aberrant network reorganization in the adult rat hippocampus. *J Neurosci*, **17**, 3727-3738.

Park, J.H., Cho, H., Kim, H. & Kim, K. (2006) Repeated brief epileptic seizures by pentylenetetrazole cause neurodegeneration and promote neurogenesis in discrete brain regions of freely moving adult rats. *Neuroscience*, **140**, 673-684.

Paxinos, G. & Franklin, K.B.J. (2001) *The Mouse Brain in Stereotaxic Cordinates, Second edition*. Academic Press, San Diego.

Platel, J.C., Heintz, T., Young, S., Gordon, V. & Bordey, A. (2008) Tonic activation of GLUK5 kainate receptors decreases neuroblast migration in whole-mounts of the subventricular zone. *J Physiol*, **586**, 3783-3793.

Suhonen, J.O., Peterson, D.A., Ray, J. & Gage, F.H. (1996) Differentiation of adult hippocampus-derived progenitors into olfactory neurons in vivo. *Nature*, **383**, 624-627.

Sundholm-Peters, N.L., Yang, H.K., Goings, G.E., Walker, A.S. & Szele, F.G. (2004) Radial glia-like cells at the base of the lateral ventricles in adult mice. *J Neurocytol*, **33**, 153-164.

Vezzani, A., Aronica, E., Mazarati, A. & Pittman, Q.J. (2011) Epilepsy and brain inflammation. *Exp Neurol*.

von Gertten, C., Holmin, S., Mathiesen, T. & Nordqvist, A.C. (2003) Increases in matrix metalloproteinase-9 and tissue inhibitor of matrix metalloproteinase-1 mRNA after cerebral contusion and depolarisation. *J Neurosci Res*, **73**, 803-810.

Walker, T.L., White, A., Black, D.M., Wallace, R.H., Sah, P. & Bartlett, P.F. (2008) Latent stem and progenitor cells in the hippocampus are activated by neural excitation. *J Neurosci*, **28**, 5240-5247.

Yu, S.W., Baek, S.H., Brennan, R.T., Bradley, C.J., Park, S.K., Lee, Y.S., Jun, E.J., Lookingland, K.J., Kim, E.K., Lee, H., Goudreau, J.L. & Kim, S.W. (2008) Autophagic death of adult hippocampal neural stem cells following insulin withdrawal. *Stem Cells*, **26**, 2602-2610.

Zhang, R.L., Zhang, Z.G., Lu, M., Wang, Y., Yang, J.J. & Chopp, M. (2006) Reduction of the cell cycle length by decreasing G1 phase and cell cycle reentry expand neuronal progenitor cells in the subventricular zone of adult rat after stroke. *J Cereb Blood Flow Metab*, **26**, 857-863.

Figure legends

Figure 1

Experimental design used to analyze cell cycle progression with immunohistochemical techniques. (A) Immediately after BrdU administration, S phase cells are BrdU+ (green), and G2/M phase cells are PH3+ (red). (B) After 3 hours, almost all PH3+ cells become BrdU+ (arrows, green and red turn to yellow; an arrowhead, PH3-only + cell). (C) After 16 hours, almost all PH3+ cells are BrdU immunonegative (-) (arrowheads, red). (D) After 18 hours, some PH3+ cells are BrdU+ (arrows, yellow; arrowheads, PH3-only + cells). Merged and stacked confocal microscopic images of the dorsolateral SVZ region are shown. CC, corpus callosum; Stri, striatum; LV, lateral ventricle. For all images, scale bar = 50 μm.

Figure 2

PTZ-induced brief seizures immediately cause transient cell cycle retardation in precursor cells in the SVZ. (A) BrdU labeling efficiency was not significantly different between the control and PTZ-treated groups 1 and 2 hours after BrdU administration.

Protocol 1 was used and average numbers of BrdU+ cells per animal were plotted. (B) The numbers of PH3+ cells per animal were not significantly different between the control and PTZ-treated groups at each time point. (C) The percentage of BrdU and PH3 double + cells among all PH3+ cells ((BrdU+, PH3+)/PH3+) was calculated using experimental protocol 1. At 1 and 2 hours, the (BrdU+, PH3+)/PH3+ ratio in the PTZ-treated group was significantly lower than that in the control group. The (BrdU+, PH3+)/PH3+ ratio decreased to about 8% at 14-16 hours after BrdU administration. At 18 hours, this value began to increase in both groups. The (BrdU+, PH3+)/PH3+ ratios were not significantly different between the control and PTZ-treated groups at 3, 4, 14, 16, 18, and 20 hours. At each time point, five mice were analyzed. Two-tailed Welch's *t*-test for all. * $P < 0.05$. White bars, control group; gray bars, PTZ-treated group; NS, not significant.

Figure 3

Cellular composition of the cycling SVZ precursors does not change after brief seizures. (A) In the SVZ, DCX (green) and EGF receptor (EGFR, red) expressions partially overlap (arrows). An arrowhead indicates a DCX-only + cell. (B) Majority of proliferating precursors (PH3+, green) are EGFR and/or DCX + cells (red) (arrows).

EGFR and DCX are visualized in red simultaneously. An arrowhead indicates a PH3-only + cell. (C) An example of PH3 (green) and GFAP (red) double + cell (an arrow). An arrowhead indicates a GFAP- proliferating cell. (D) Virtually there is no PH3 and Iba1 double + cell 22 hours after PTZ administration. Arrowheads indicate PH3-only + cells (green). (E) Cellular composition of proliferating cells in the SVZ after brief seizures did not change. One-way ANOVA for all. At each time point, five animals were analyzed. Single optical confocal microscopic images taken from the control (A-C) and the PTZ-22 hour (D) mouse are shown. For all images, scale bar = 50 μm.

Figure 4

PTZ-induced seizures have no effect on the cell cycling of SGZ precursors immediately after brief seizures. (A) Experimental design used to analyze cell cycle progression with the double thymidine analogue labeling technique (experimental protocol 2). IdU-labeled cells pass through S phase and a new population of cells enter S phase over time. With the second administration of BrdU, all S phase cells are labeled with BrdU. Rat monoclonal anti-BrdU antibody (clone BU1/75) recognizes BrdU but not IdU, and mouse monoclonal anti-BrdU antibody (clone B44) recognizes both BrdU and IdU.

Thus, the ratio of IdU-only + cells (black) to all + cells (IdU-only+, IdU and BrdU double +, and BrdU-only + cells; black and hatched) increases to about 50% with cell cycle progression. (B) The IdU-only +/all + ratio increased over time, but there was no significant difference between the control and PTZ-treated groups. At each time point, four mice were analyzed. Two-tailed Welch's *t*-test. White bars, control group; gray bars, PTZ-treated group.

Figure 5

Precursor proliferation is transiently enhanced 3 days after PTZ-induced seizures in the SGZ. (A) The total number of Ki67+ cells was significantly higher in the PTZ-treated group than in the control group 3 days after seizures. At each time point, five mice were analyzed. Two-tailed Welch's *t*-test. $^{**}P < 0.01$. White bars, control group; gray bars, PTZ-treated group. (B) There are more Ki67+ cells (arrows) in the PTZ-treated mouse 3 days after seizures than in the control mouse. Stacked confocal microscopic images of the dentate gyrus are shown. Dotted line, SGZ; GrD, granular layer of the dentate gyrus. Scale bar = 100 μm.

Figure 6

Precursor pool in the SVZ transiently expands after brief seizures by enhancing cell cycle re-entry. (A) Experimental design used to analyze cell cycle re-entry. BrdU (green) and Ki67 (red) immunostaining can be used to detect cells that have exited the cell cycle. At the 20-hour time point after BrdU administration, cells that have exited the cell cycle are BrdU+ and Ki67- (green, arrowheads), but cells that have re-entered the cell cycle are BrdU+ and Ki67+ (yellow, arrows). Merged and stacked confocal microscopic images of the dorsolateral SVZ region are shown. (B) The percentage of Ki67 and BrdU double + cells among all BrdU+ cells ((Ki67+, BrdU+)/BrdU+) 20 hours after seizures was calculated using experimental protocol 1. The (Ki67+, BrdU+)/BrdU+ ratio in the PTZ-treated group (n = 5) was significantly higher than that in the control group (n = 6). (C) The total number of Ki67+ cells was also significantly higher in the PTZ-treated group than in the control group (n = 5). (D) The numbers of PH3+ cells were followed after 20 hours. At 22 and 26 hours, the number of PH3+ cells in the SVZ increased significantly in the PTZ-treated group, but returned to the control level after 30 hours (n = 5 at each time point). (E) The size of the precursor pool was estimated using experimental protocol 3. There was no significant difference in the total number of BrdU+ cells between the control and PTZ-treated groups at 2 and 4 days after seizures (n = 5 at each time point). Two-tailed Welch's t-test for all. *$P < 0.05$, **P

< 0.01. White bars, control group; gray bars, PTZ-treated group. Scale bar = 50 μm.

Figure 7

PTZ-induced seizures have no effect on migration of precursors from the SVZ to the OB. Experimental protocol 1 was used to count the number of BrdU+ cells in the GrO. BrdU+ cells migrate and accumulate in the core of OB over time after BrdU administration. There are few BrdU+ cells (white dots) at 4 hours (A), but at 3 days there are many BrdU+ cells in the core of the OB (B). Then BrdU labeled precursors migrate out from the core of the OB (C). Epifluorescent microscopic images are shown. (D) The total number of BrdU+ cells was not significantly different between the control and PTZ-treated groups 3 and 7 days after treatment (n = 4). Two-tailed Welch's t-test. White bars, control group; gray bars, PTZ-treated group. Arrows, the core of the OB; Gl, glomerular layer; GrO, granular layer of the OB. Scale bar = 300 μm.

Figure 8

Seizures have no effect on the fate of precursors. The number of new cells in the OB 4 weeks after seizures was analyzed using experimental protocol 1 (A and B) and protocol 4 (C). The total number of BrdU+ cells (A, n = 4) and the percentage of NeuN and

BrdU double + cells among all BrdU+ cells ((NeuN+, BrdU+)/BrdU+) (B, $n = 4$) were not significantly different between the control and PTZ-treated groups. (C) Surplus precursors were labeled by BrdU after brief seizures and followed their fate. There was no significant difference between the control and PTZ-treated groups in the total number of BrdU, and the number of BrdU+ cells in the GrO and in the Gl ($n = 3$). Two-tailed Welch's *t*-test for all. White bars, control group; gray bars, PTZ-treated group.

Figure 9

ECS has similar effects to PTZ-induced seizures on SVZ precursors. The effects of ECS were examined using experimental protocol 5. (A) At 2 hours, the percentage of (BrdU+, PH3+)/PH3+ in the ECS group ($n = 5$) was lower than that in the control group. (B) At 20 hours, the (Ki67+, BrdU+)/BrdU+ ratio in the ECS group ($n = 5$) was significantly higher than that in the control group. The value in the control group is shown again for comparison (see also Figures 2C and 6B). Two-tailed Welch's *t*-test for all. $^{*}P < 0.05$, $^{**}P < 0.01$. White bars, control group; dark gray bars, ECS group.

Supplemental Figure 1

PTZ-induced brief seizures do not significantly induce apoptosis. (A) TUNEL+ cells (red) in the control SVZ (arrows). Nuclei are visualized with Hoechst33258 (light blue). Stacked confocal microscopic images are shown. (B) There was no significant difference in the number of TUNEL+ cells between the control and PTZ-treated group 36 hours after seizures. Scale bar = 50 μm.

Supplemental Figure 2

Cell cycle analysis with double thymidine analogue labeling in the SGZ. Experimental protocol 2 was used. The ratio of IdU-only + cells (arrowheads) among all + cells (red, IdU-only + cells, IdU and BrdU double + cells, and BrdU-only + cells) increase from 3 hours (A) to 6 hours (B). Arrows indicate IdU and BrdU double + cells. Stacked confocal microscopic images are shown. Dotted line, SGZ; GrD, granular layer of the dentate gyrus. Scale bar = 100 μm.

Supplemental Figure 3

BrdU labeled precursors differentiate into mature neurons in the OB after 4 weeks.

(A) BrdU + cells (white dots) migrate to the GrO and Gl in the control (left column) and

the PTZ-treated mouse (right column). Epifluorescent microscopic images are shown. (B) BrdU+ cells express NeuN, a maker for mature neurons, in the GrO (left column) and the Gl (right column). Arrows indicate BrdU and NeuN double + cells. Single optical confocal microscopic images are shown. (C) Examples of the morphology of BrdU (green) and calretinin (CR, red) double + mature granular neurons (arrows). Their morphologies in the control (left column) and PTZ-treated (right column) group are similar to each other. Arrowheads indicate long processes extending toward the outer layer. Stacked confocal microscopic images are shown. Scale bar = 300, 50, and 20 μm for A, B, and C respectively.

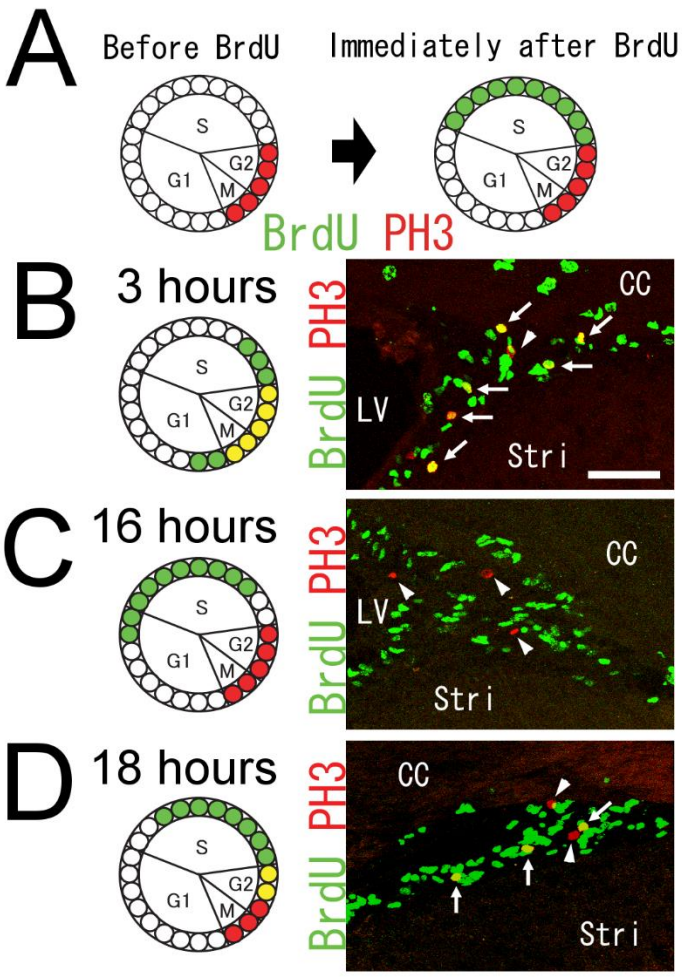
A
Before BrdU
Immediately after BrdU
S
G2
G1
M
BrdU PH3
B
3 hours
BrdU PH3
CC
LV
Stri
C
16 hours
BrdU PH3
CC
LV
Stri
D
18 hours
BrdU PH3
CC
Stri

Figure 1

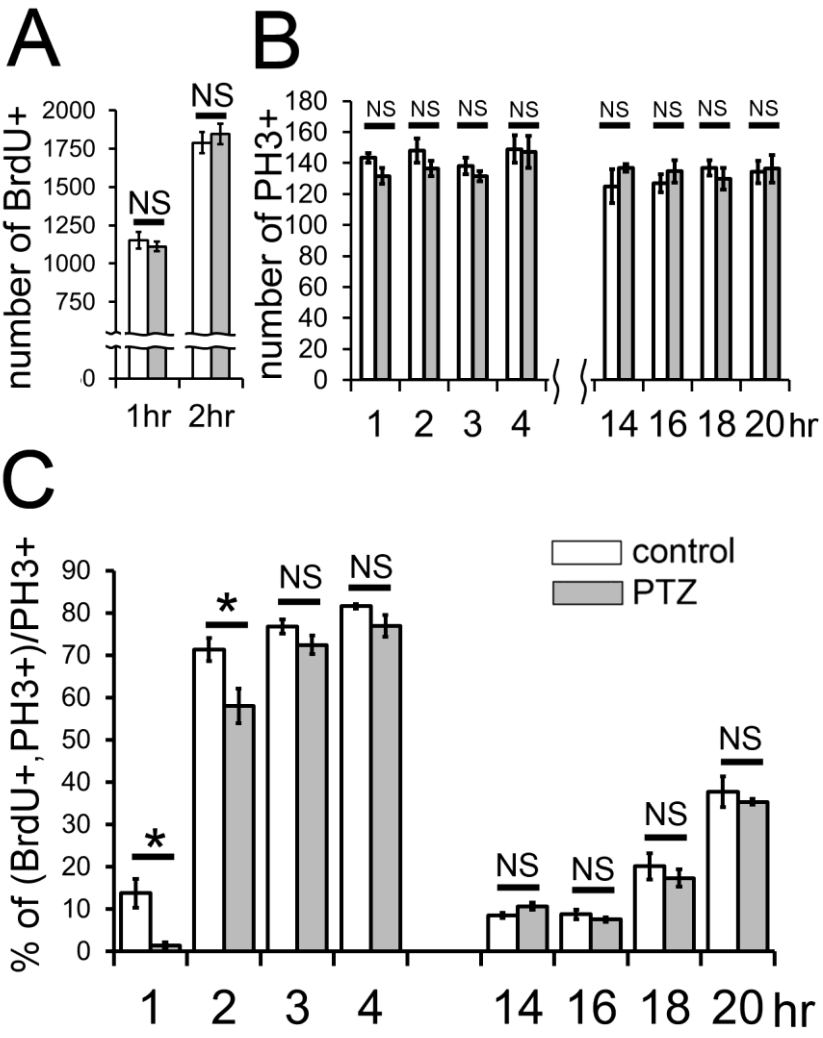
A
B
number of BrdU+
2000
1750
1500
1250
1000
750
0
NS
NS
1hr
2hr
number of PH3+
180
160
140
120
100
80
60
40
20
0
NS
1
2
3
4
14
16
18
20hr
C
% of (BrdU+,PH3+)/PH3+
90
80
70
60
50
40
30
20
10
0
control
PTZ
*
*
NS
NS
NS
NS
NS
NS
1
2
3
4
14
16
18
20 hr

Figure 2

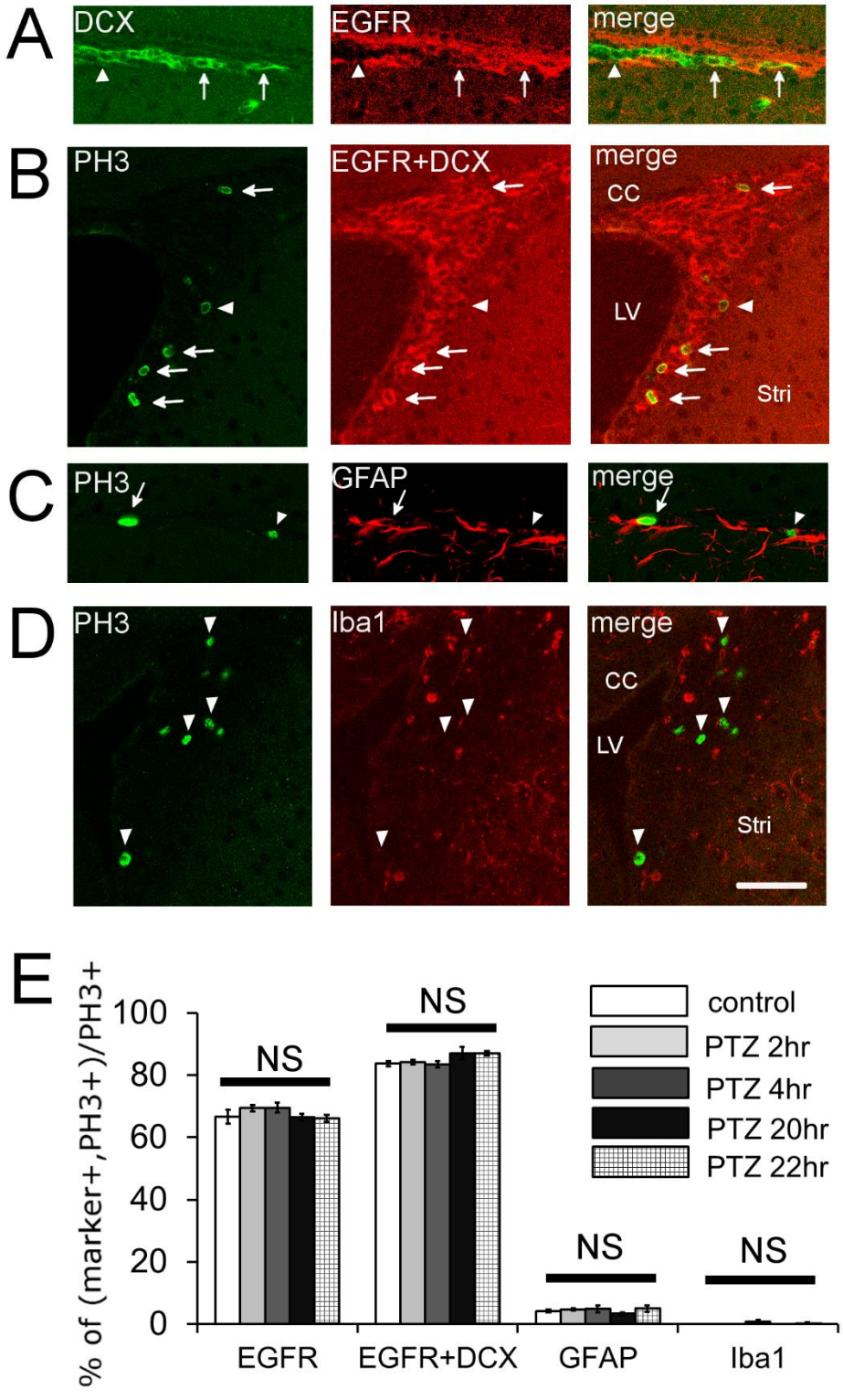
A
DCX
EGFR
merge
B
PH3
EGFR+DCX
merge
cc
LV
Stri
C
PH3
GFAP
merge
D
PH3
Iba1
merge
cc
LV
Stri
E
% of (marker+,PH3+)/PH3+
100
80
60
40
20
0
NS
NS
NS
NS
control
PTZ 2hr
PTZ 4hr
PTZ 20hr
PTZ 22hr
EGFR
EGFR+DCX
GFAP
Iba1

Figure 3

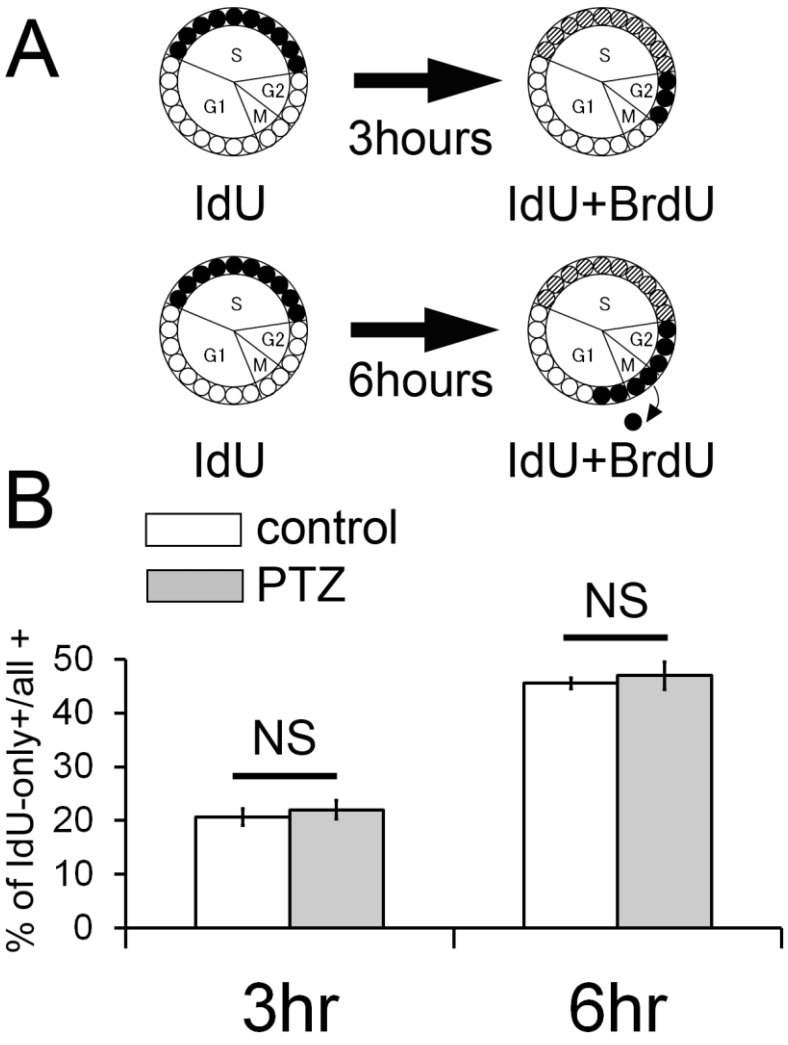
A
S
G2
G1
M
3hours
IdU
IdU+BrdU
6hours
B
control
PTZ
NS
NS
% of IdU-only+/all +
50
40
30
20
10
0
3hr
6hr

Figure 4

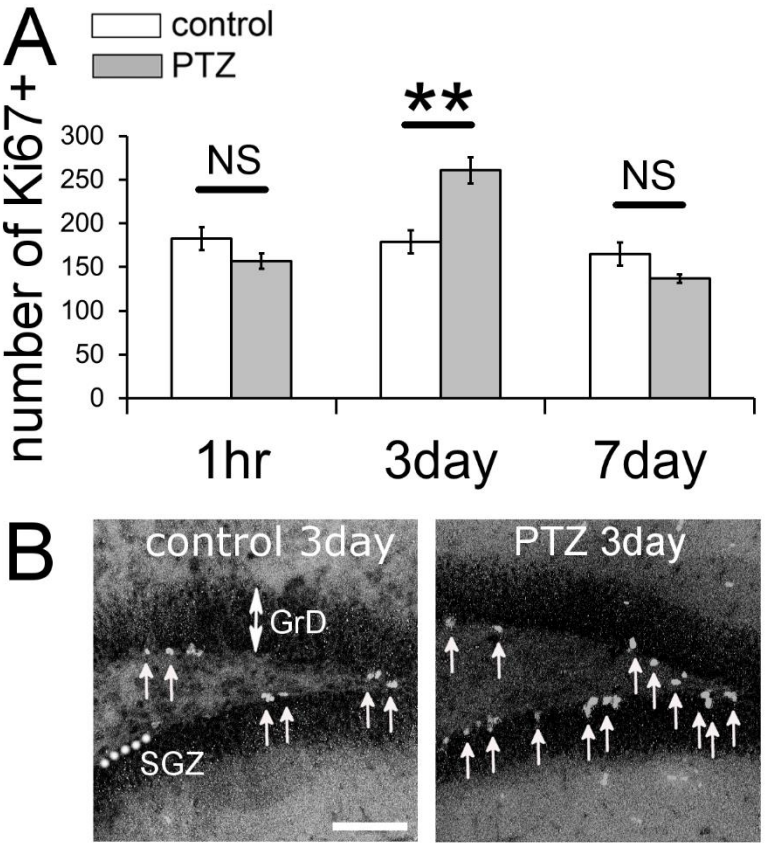
A
control
PTZ
number of Ki67+
300
250
200
150
100
50
0
NS
**
NS
1hr
3day
7day
B
control 3day
GrD
SGZ
PTZ 3day

Figure 5

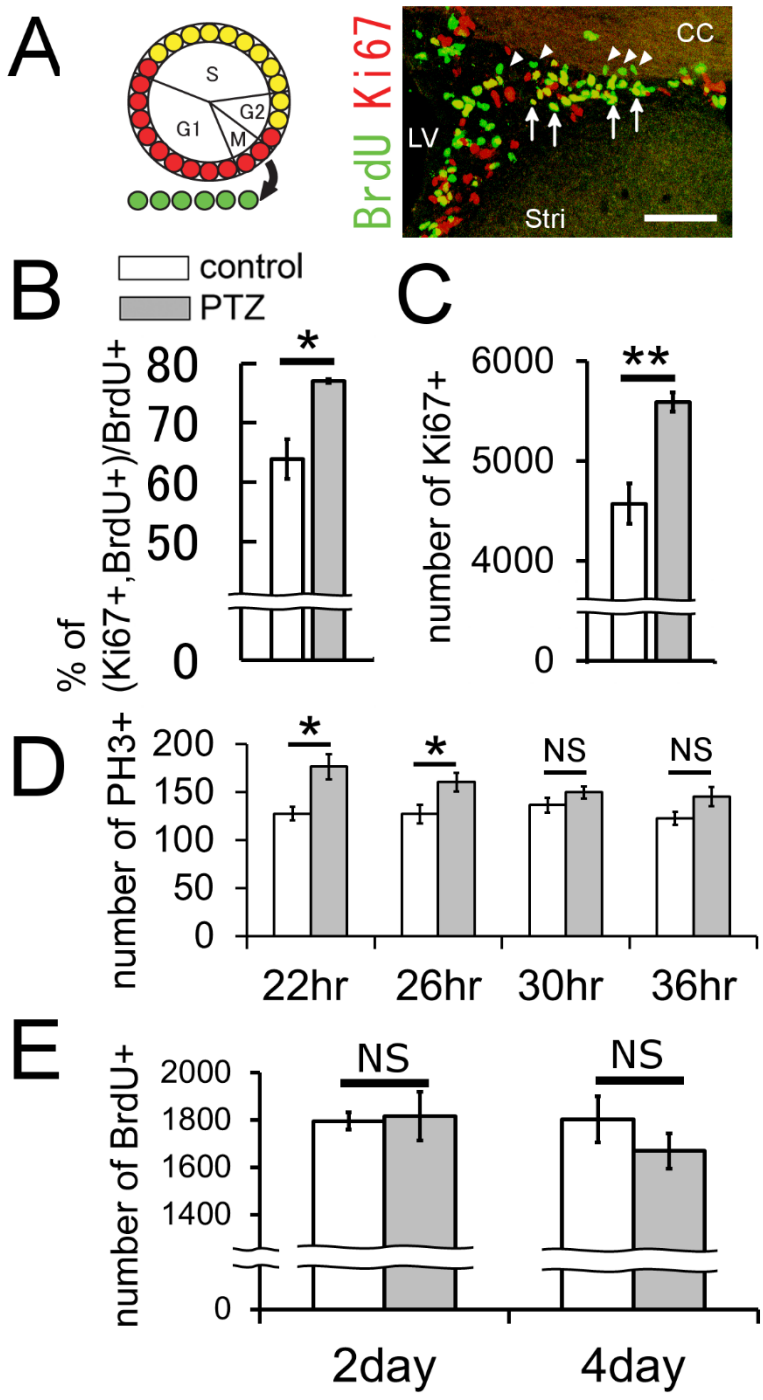
A
S
G2
G1
M
BrdU Ki67
CC
LV
Stri
B
control
PTZ
% of (Ki67+,BrdU+)/BrdU+
80
70
60
50
0
*
C
number of Ki67+
6000
5000
4000
0
**
D
number of PH3+
200
150
100
50
0
*
*
NS
NS
22hr
26hr
30hr
36hr
E
number of BrdU+
2000
1800
1600
1400
0
NS
NS
2day
4day

Figure 6

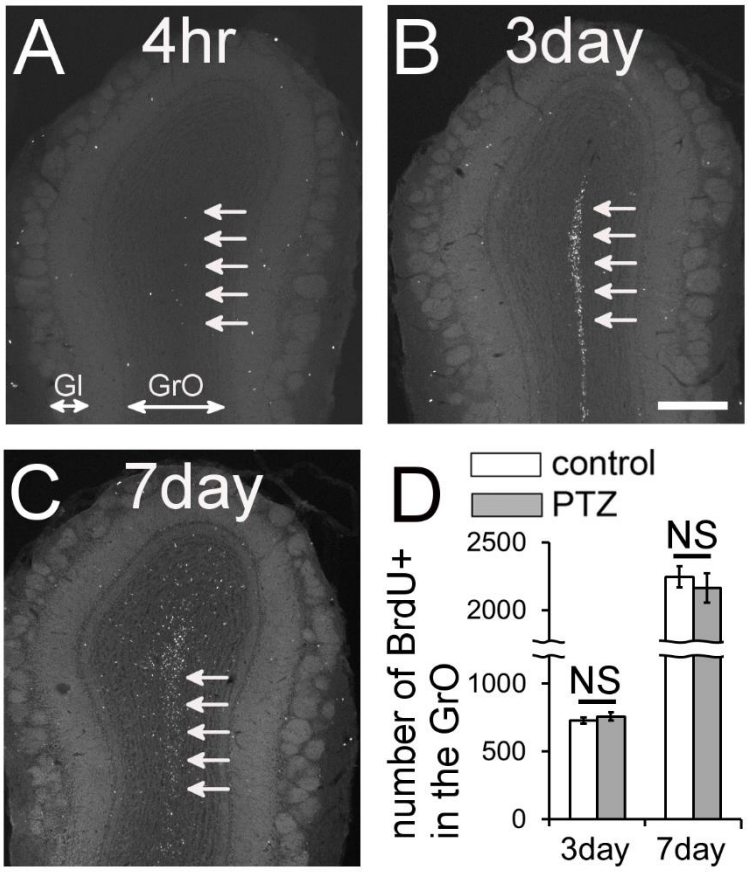
A
4hr
GI
GrO
B
3day
C
7day
D
control
PTZ
number of BrdU+ in the GrO
2500
2000
1000
500
0
NS
NS
3day
7day

Figure 7

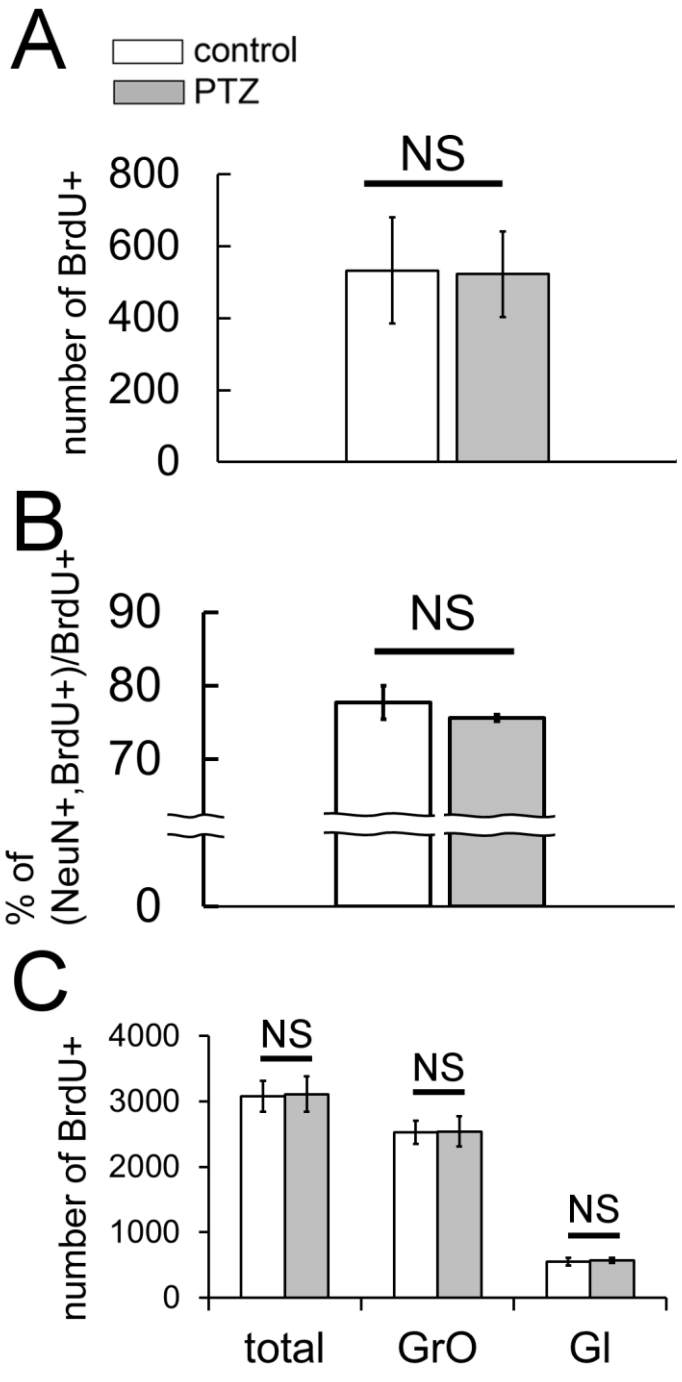
A
control
PTZ
NS
number of BrdU+
800
600
400
200
0
B
NS
% of (NeuN+,BrdU+)/BrdU+
90
80
70
0
C
NS
NS
NS
number of BrdU+
4000
3000
2000
1000
0
total
GrO
Gl

Figure 8

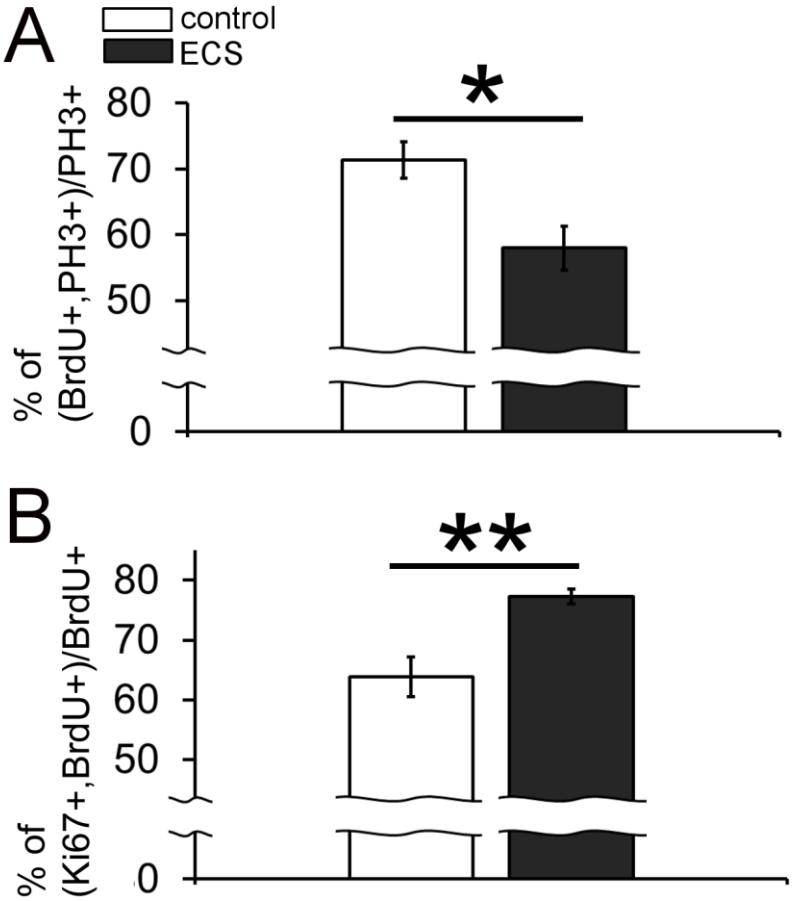
A
control
ECS
*
80
70
60
50
0
% of (BrdU+,PH3+)/PH3+
B
**
80
70
60
50
0
% of (Ki67+,BrdU+)/BrdU+

Figure 9

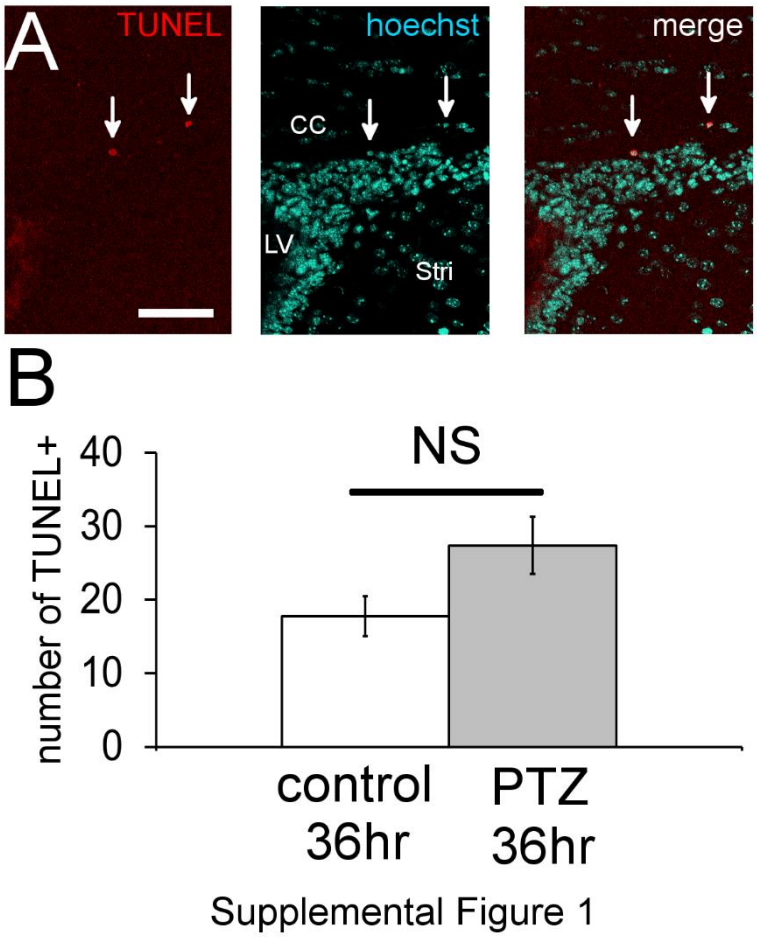

Supplemental Figure 1

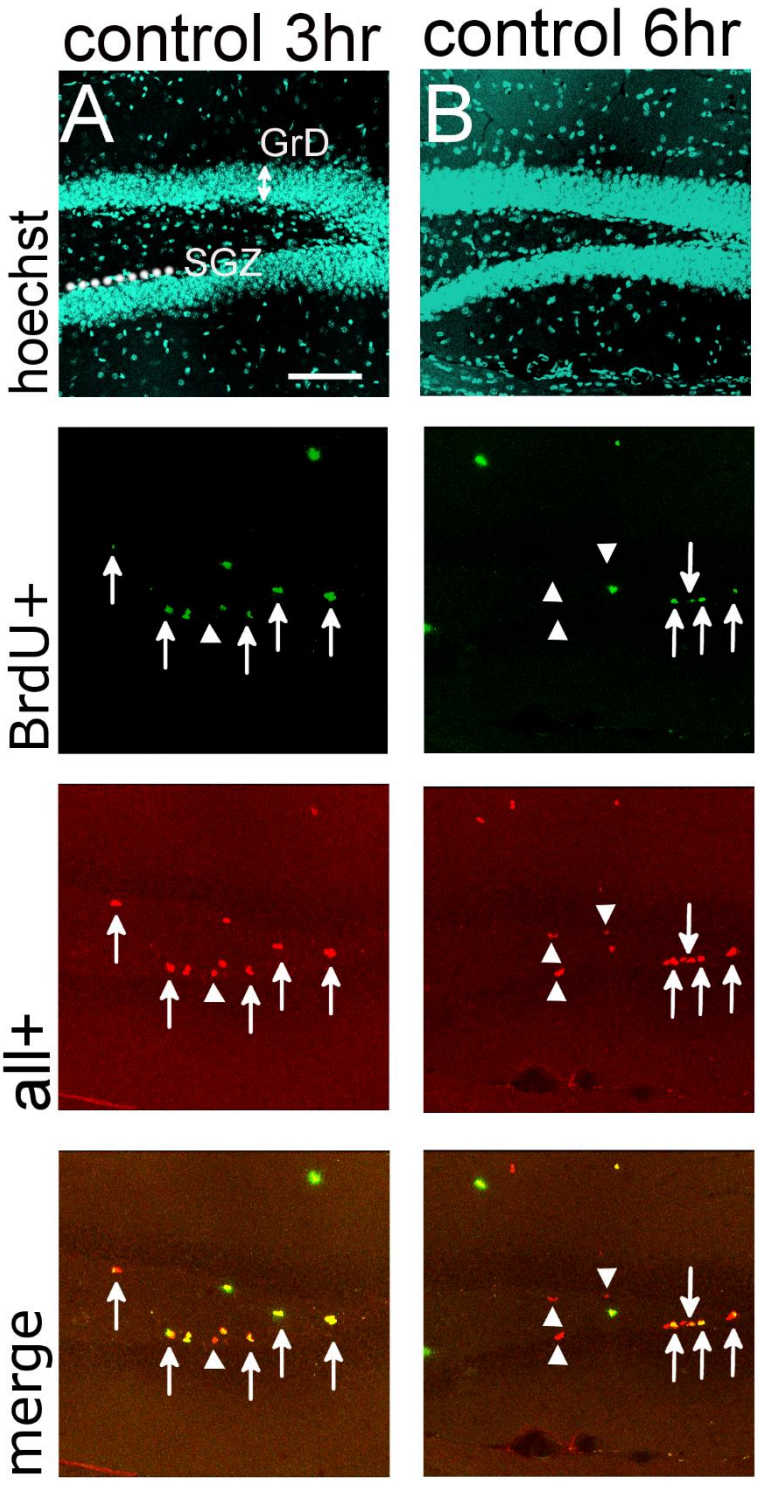

Supplemental Figure 2

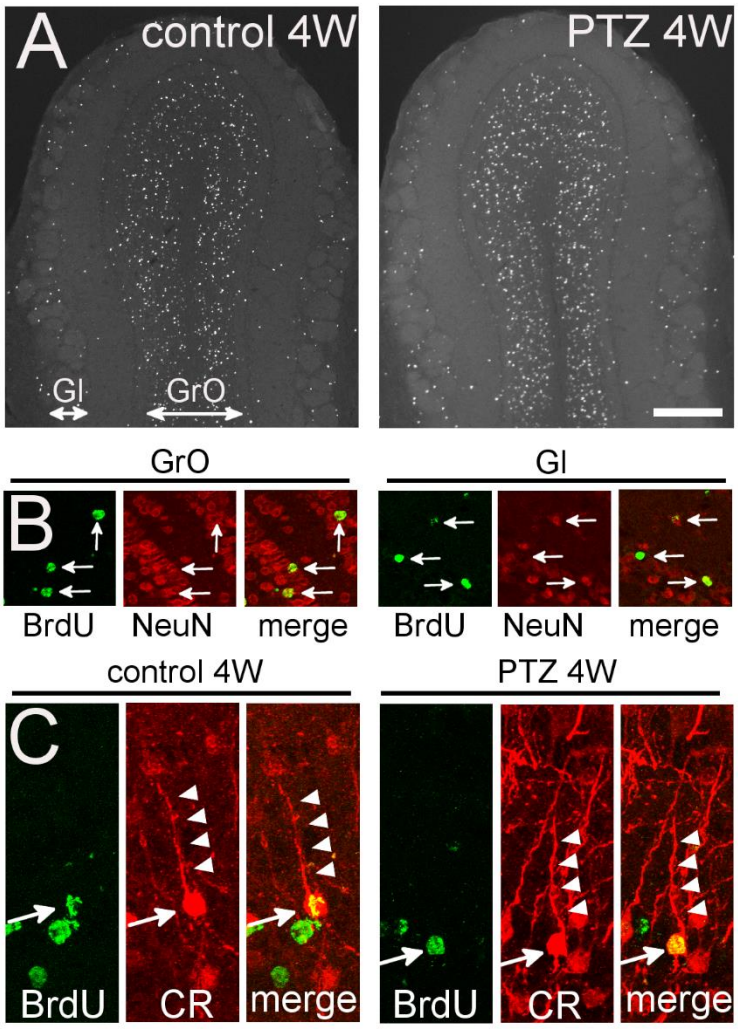

Supplemental Figure3